Catalyst-Controlled Intermolecular Homobenzylic C(sp 3)–H Amination for the Synthesis of β-Arylethylamines

Erwan Brunard, Vincent Boquet, Tanguy Saget, E. Daiann Sosa Carrizo, Marie Sircoglou, Philippe Dauban

Catalyst-Controlled Intermolecular Homobenzylic C(sp^3)–H Amination for the Synthesis of β-Arylethylamines

Erwan Brunard,[a] Vincent Boquet,[a] Tanguy Saget,[a] E. Daiann Sosa Carrizo,*[,b] Marie Sircoglou,*[,b] and Philippe Dauban*[,a]

[a] Université Paris-Saclay, CNRS, Institut de Chimie des Substances Naturelles, UPR 2301, 91198 Gif-sur-Yvette, France.

[b] Université Paris-Saclay, CNRS, Institut de Chimie Moléculaire et des Matériaux d'Orsay, 91405 Orsay, France.

ABSTRACT: The combination of a tailored sulfamate with a C_4-symmetrical rhodium(II) tetracarboxylate allows to uncover a selective intermolecular amination of unactivated homobenzylic C(sp^3)–H bonds. The reaction has a broad scope (>30 examples) and proceeds with a high level of regioselectivity with homobenzylic:benzylic ratio of up to 35:1, thereby providing a direct access to β-arylethylamines that are of utmost interest in medicinal chemistry. Computational investigations evidence a concerted mechanism, involving an asynchronous transition state as key intermediate. Based on a combined activation strain model and energy decomposition analysis, the regioselectivity of the reaction was found to rely mainly on the degree of orbital interaction between the [Rh$_2$]-nitrene and the C–H bond. The latter is facilitated at the homobenzylic position due to the establishment of specific non-covalent interactions within the catalytic pocket.

INTRODUCTION

Catalytic C(sp^3)–H functionalization reactions are revolutionizing the art of organic synthesis. The ability to directly convert unactivated C(sp^3)–H bonds into functional groups provides new avenues for retrosynthetic analysis, with bond disconnections allowing the design of step-economical synthetic strategies.[1] In the context of late-stage diversification of drug candidates, C(sp^3)–H functionalization reactions are of paramount importance to give streamlined access to new derivatives that it would be time-consuming, or even impossible, to prepare using classical organic reactions. The ubiquity of C–H bonds in organic chemistry makes them ideal starting points to explore new molecular spaces provided that orthogonal conditions are available for the selective conversion of every type of C–H bonds.[2]

The selective functionalization of a specific methylene unit within linear alkyl chains fits perfectly into this objective of step economy and new molecular diversity; however, it remains one of the most challenging transformations to achieve in intermolecular C(sp^3)–H functionalization reactions.[3] Linear alkyl chains indeed possess multiple secondary C(sp^3)–H bonds of very similar electronic and steric properties, making their chemical differentiation notoriously highly difficult, although innate factors might favor the functionalization of one particular methylene unit.[4] In this context, a textbook case is provided by the arylalkyl motif that undergoes selective functionalization reactions at the benzylic C(sp^3)–H bond as a result of its lower bond dissociation energy (BDE 85 kcal.mol^{-1}) (Scheme 1a).[5] It has been shown that the design of reagents and catalysts can overcome such substrate-controlled selectivity. For example, the steric and/or the electronic properties of metal-carbenes, -nitrenes, and -oxos species are known to afford selectivities that are not driven by the BDE's.[6] Among those examples and in the context of our study, Davies reported a sterically demanding rhodium(II) complex for the selective carbene C–H insertion at the terminal methylene unit of arylpentane (Scheme 1b).[6b]

In the same manner, the use of weak non covalent interactions to direct the relative positioning of the substrate and the catalyst proved to be a versatile strategy to tune the selectivity of a reaction.[7] This elegant strategy pioneered by Breslow[8] was applied to the site-selective oxidation of C–H bonds.[9] Particularly

Scheme 1. Selective Functionalization of Arylalkyl Motifs

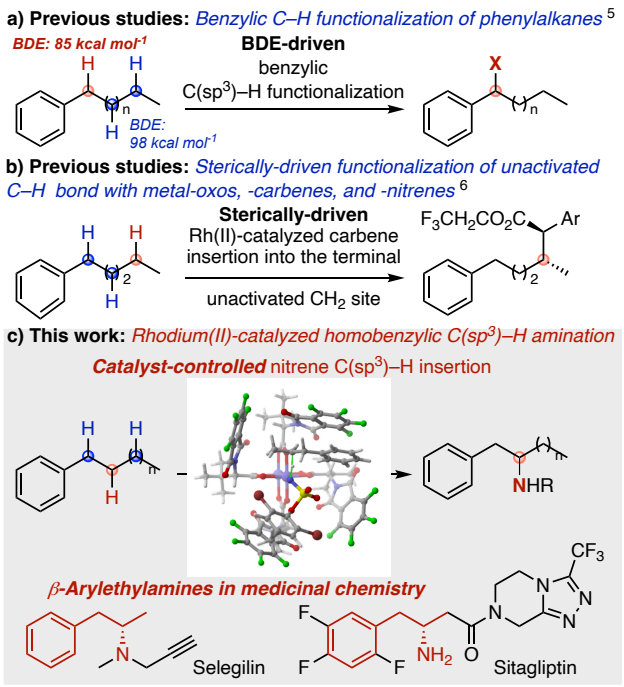

recent contributions from the groups of Costas and Tiefenbacher demonstrated that supramolecular complexes can be designed for the catalyst-controlled selective oxidation of linear alkyl chains.[10] A similar supramolecular approach was used to address the issue of enantioselectivity in intermolecular C(sp^3)–H amination reactions.[11] However, these directed reactions proceed selectively at the more activated benzylic site, as observed in catalytic nitrene C(sp^3)–H insertions.[12] Nevertheless, seminal investigations in catalyst-controlled C(sp^3)–H functionalization processes suggest that a directing effect could be envisaged to go beyond the innate reactivity of benzylic sites towards nitrene species.[13] Non-covalent interactions in particular might be appropriate to tune the site-selectivity of intermolecular C(sp^3)–H amination and favor the formation of the C–N bond at the homobenzylic position of a linear alkyl chain. If successful, such

a process would afford β-arylethylamines, which are a pharmacophore of utmost importance in medicinal chemistry (Scheme 1c).[14] For example, the arylethylamine motif forms the core of CNS acting agents such as Selegilin, or metabolic agents such as Sitagliptin. Classical synthetic methods for their preparation rely on functional group transformations such as reductive amination or alkene hydroamination.[15] In comparison, the direct intermolecular amination of arylalkyl motifs could offer a new bond disconnection for the synthesis of arylethylamines. In this communication, we thus describe such a novel approach by the discovery of a sulfamate-derived rhodium-bound nitrene that allows the selective C(sp^3)–H amination of homobenzylic methylene sites directed by non-covalent interactions.

RESULTS AND DISCUSSION

Searching for conditions favoring the catalytic homobenzylic C(sp^3)–H amination. Chiral rhodium(II) complexes, that display C_2-, D_2-, or C_4-symmetries according to the structure of the carboxylate ligand, are exquisite catalysts for selective carbene and nitrene C–H insertions. It is worth noting that the site-selectivity of the reaction can be tuned by both the geometry of the tetracarboxylate complexes and the structure of the carbene or nitrene precursors.[16] For the catalytic C–H amination reaction, the combination of rhodium(II) complexes with sulfamates was found optimal to efficiently catalyze the selective functionalization of C(sp^3)–H bonds.[17] On the one hand, chiral C_4-symmetrical rhodium(II) tetracarboxylates proved to be unique catalysts owing to their tunable hydrophobic pocket (Figure 1). The latter delineates a confined environment in which the nitrene addition can be directed as shown in the case of alkene aziridination.[18] On the other hand, according to the nature of the sulfamate, it was possible to selectively functionalize either a benzylic (B) or a tertiary (T) C(sp^3)–H bond.[17c,e] Based on these results, we decided to search for an appropriate combination of a rhodium(II) complex and a sulfamate to address the challenge of the selective homobenzylic (H) C–H amination.

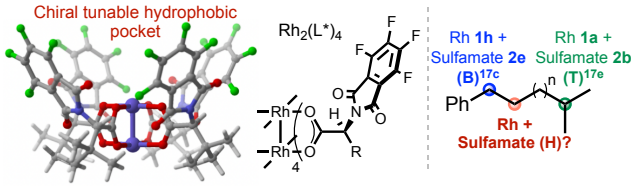

Figure 1. C_4-Symmetrical Dirhodium(II) Tetracarboxylate Catalysts and Sulfamates

Our investigations started with the screening of sulfamates to perform the selective homobenzylic amination of 1-phenylpropane **3a** in the presence of the chiral complex dirhodium(II) tetrakis[*N*-tetrafluorophthaloyl-(*S*)-*tert*-leucinate] (Rh_2(*S*-tfpttl)$_4$) **1a** (Scheme 2). The use of sulfamate TBPhsNH$_2$ **2b** under the conditions reported for the selective amination of tertiary C(sp^3)–H bonds[17e] led to the isolation of the homobenzylic amine with a H:B ratio of 3:1. Then, we screened other sulfamates **2c-f**[17a-d] that were previously described for intermolecular C–H amination reactions but without significant success; the benzylic amine was often formed in major quantity. Reduced levels of H:B selectivity were also observed upon modification of the *para* substitution (**2g** and **2h**; see also SI Scheme S1) whereas the presence of substituents at the *meta* position favored the amination of the benzylic center (**2i**). Therefore, we turned our attention to the *ortho* substituents which proved to

Scheme 2. Screening of Sulfamates with the Rh_2(*S*-tfpttl)$_4$ Complex 1a.

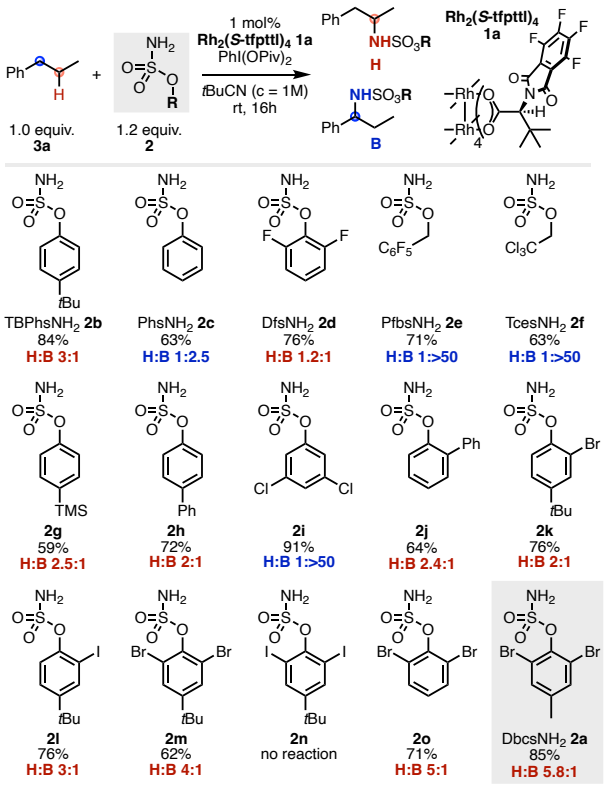

Scheme 3. Screening of Chiral Rhodium(II) Complexes with DbcsNH$_2$ 2a.

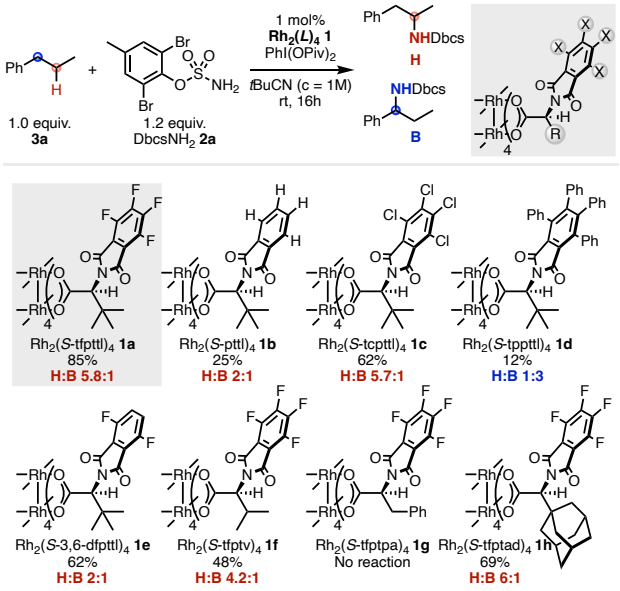

be important to promote the formation of homobenzylic amines. An improved H:B ratio of 4:1 was obtained following the introduction of a bromo substituent at both *ortho* positions of the aromatic ring (**2m**). More significantly, the replacement of the *para* *t*-butyl group by a smaller methyl substituent increased both the yield and the selectivity. Accordingly, the 2,6-dibromocresolsulfonamide (DbcsNH$_2$) **2a** afforded the homobenzylic amine with an H:B ratio of 5.8:1 (85% yield for the mixture of homobenzylic and benzylic amines).

Scheme 4. Screening of the Iodine(III) Oxidant.

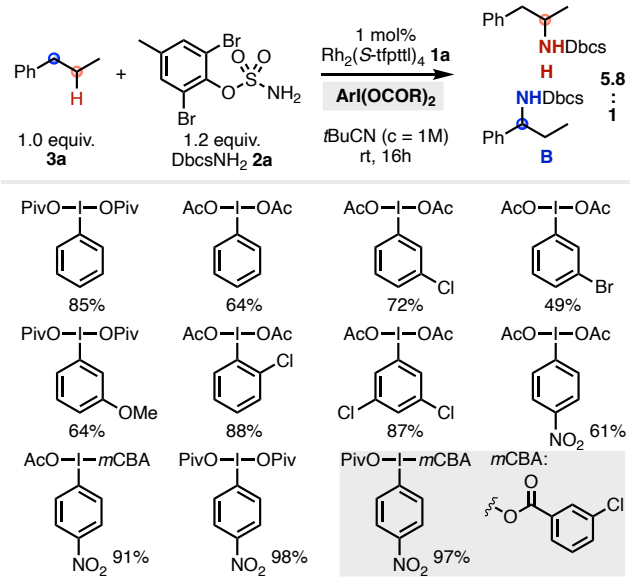

Sulfamate **2a** was therefore chosen to further optimize the conditions. We then screened the amino acid ligands of the rhodium(II) tetracarboxylate catalyst **1** (Scheme 3). For the *N*-phthaloyl protecting group, the presence of the perfluorinated aromatic ring was found crucial to secure both a high yield and a good H:B ratio (**1a** *vs.* **1b-d**). The four fluorine substituents are necessary to this end as the 3,6-difluoroaryl motif (**1e**) led to a reduced yield of 62% and a H:B ratio of 2:1. With respect to the side chain of the amino acid, the *t*-butyl group gave the best compromise between reactivity and selectivity. Particularly, although the adamantyl-derived complex **1h** afforded a slightly higher H:B ratio of 6:1 compared to **1a**, the yield of 69% was much lower than the one obtained with the *t*-butyl complex **1a** (85%).

The subsequent screening of the iodine(III) oxidant using sulfamate **2a** and rhodium(II) complex **1a** revealed a critical influence of this reagent on the reactivity, a key result not only related to the carboxylate ligand but also to the iodoarene moiety (Scheme 4). Whereas the replacement of $PhI(OPiv)_2$ by $PhI(OAc)_2$ decreased the yield by approximately 20%, the introduction of chloro substituents[19] on the iodoarene ring could restore the initial reactivity. More interestingly, while the *p*-nitro-iodobenzene(diacetate)[20] allowed us to isolate the homobenzylic amine in 61% yield, the use of an analog having a *m*-chlorobenzoic acid ligand (*m*CBA)[21] gave the same product with an improved yield of 91%. Replacing the acetate by a pivalate ligand proved beneficial and delivered the homobenzylic compound in 97% yield with the same H:B ratio of 5.8:1. The bis(pivaloyloxy) analog proved to be as efficient (98% yield) but its more tedious preparation led us to choose the *p*-$NO_2C_6H_4I(OPiv)(m$CBA) reagent as the optimal oxidant.

The fact that the carboxylate ligand has an influence on the efficiency of the C–H amination reaction is not unprecedented as demonstrated by the group of Du Bois.[22] In contrast and to the best of our knowledge, the non-innocent role of the iodoarene moiety on the course of iodine(III) oxidant-mediated nitrene transfer reactions has not been documented so far.[23] In a seminal paper on the mechanism of catalytic alkene aziridination, the group of Jacobsen concluded on the absence of any influence of the iodoarene part.[24] However, this work involved the use of

Scheme 5. Catalytic Homobenzylic C(sp^3)–H Amination of 1-Arylpropanes.[a]

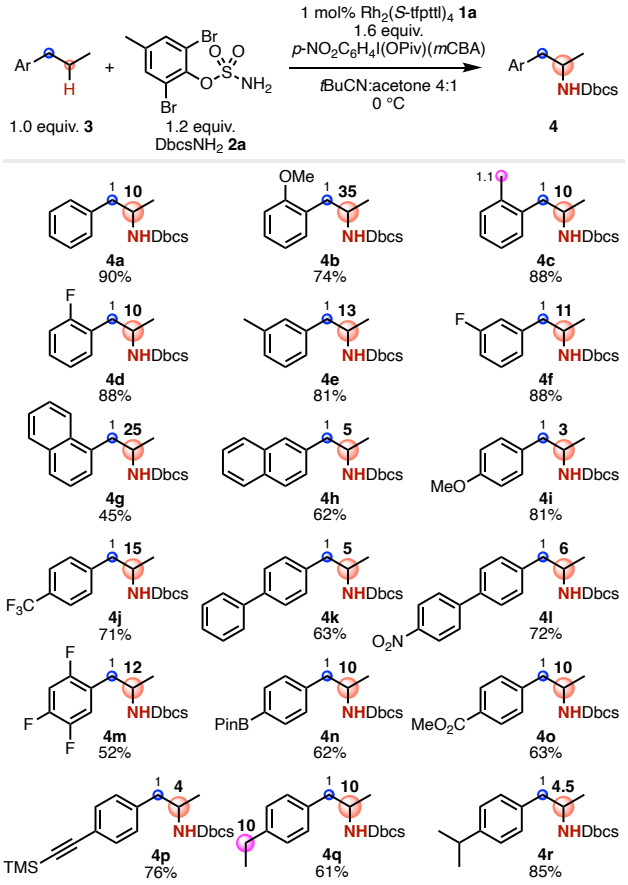

[a] Reaction conditions: substrate (0.3 mmol), sulfamate **2a** (0.36 mmol), iodine oxidant (0.48 mmol), and rhodium catalyst **1a** (1 mol%) in *t*BuCN:acetone 4:1 (0.6 mL) at 0 °C. The yields are fo

preformed iminoiodinanes. More recently, the *in situ* formation of the latter was shown by Du Bois to be rate-limiting, at least in the early stage of the rhodium-catalyzed intramolecular C–H amination.[6d,25] This hypothetical mechanistic scenario could suggest that the increased reactivity observed with the *p*-nitro-iodoarene motif might result from an easier generation of the corresponding iminoiodinane.

A final screening of reaction parameters such as the temperature and the amount of the iodine(III) oxidant or the rhodium complex **1a** (SI Tables S1, S2, and S3) further improved the regioselectivity of the amination. Thus, the homobenzylic amine derived from 1-phenylpropane was isolated with a H:B ratio of 10:1 (90% yield for the mixture of homobenzylic and benzylic amines) by performing the reaction in a 4:1 mixture of pivalonitrile:acetone at 0 °C, using 1.6 equivalent of *p*-$NO_2C_6H_4I(OPiv)(m$CBA)[26] in the presence of 1 mol% of the rhodium complex **1a**.

Scope of the rhodium(II)-catalyzed homobenzylic C–H amination. At first, the scope of the homobenzylic C(sp^3)–H amination reaction first focused on 1-arylpropanes used in stoichiometric amounts (Scheme 5). The optimal conditions proved to deliver the homobenzylic amines with high yields (from 45 to 90% for the mixture) and excellent H:B ratios of up to 35:1. Particularly high regioselectivities were observed with substrates having an *ortho* substituent (**4b-d**, **4g**) that further prevents the reaction to proceed at the benzylic position due to

Scheme 6. Catalytic Homobenzylic C(sp^3)–H Amination of Functionalized Arylalkanes

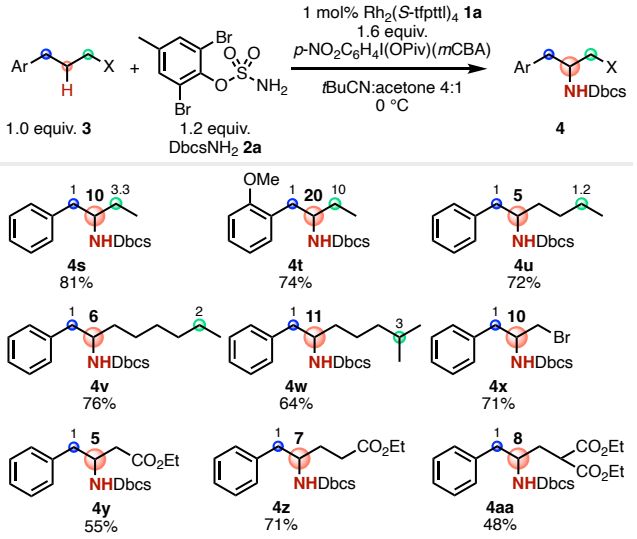

Scheme 7. Catalytic Homobenzylic C(sp^3)–H Amination of 1,n-Diarylalkanes

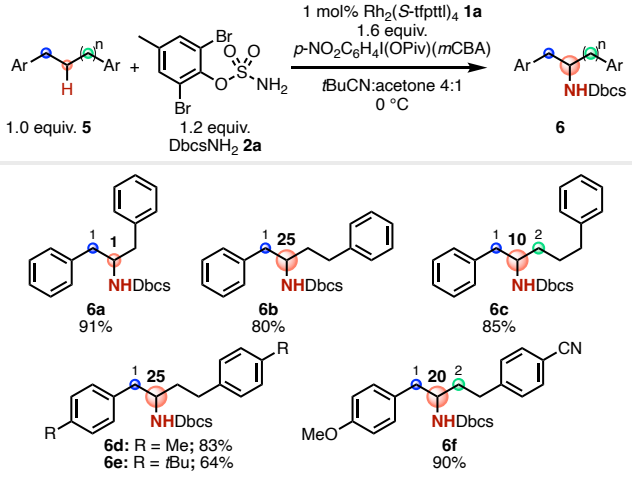

steric reasons in addition to the control provided by the rhodium-nitrene species. In the case of *p*-substituted derivatives (**4i-4l** and **4n-4r**), the regioselectivity was found to depend also on electronic factors. For example, while a H:B ratio of 15:1 could be obtained in the case of the trifluoromethyl analog **4j**, a reduced ratio of 3:1 was observed with the *p*-methoxy derivative **4i** that possesses more electron rich benzylic position. In terms of chemoselectivity, the reaction tolerates the presence of either an electron-donating group (alkyl, aryl, alkynyl, methoxy) or an electron-withdrawing group (fluoro, trifluoromethyl, ester, boronic acid) at any position of the aromatic ring. Finally, whereas the reaction proceeded selectively at the homobenzylic position in the case of the *i*-propyl analog **4r**, the presence of a *p*-ethyl substituent led to a 1:1 mixture of the homobenzylic amine **4q** and the benzylic amine resulting from the functionalization of the ethyl substituent that is known to be highly reactive in catalytic intermolecular C(sp^3)–H aminations.[12]

We then turned our attention to more challenging derivatives having a longer alkyl chain (Scheme 6). Application of the reaction conditions to 1-arylbutane derivatives (**3s** and **3t**), 1-phenylhexane **3u** and 1-phenyloctane **3v** led to the highly selective

Scheme 8. Gram-Scale Synthesis of Homobenzylic Amine

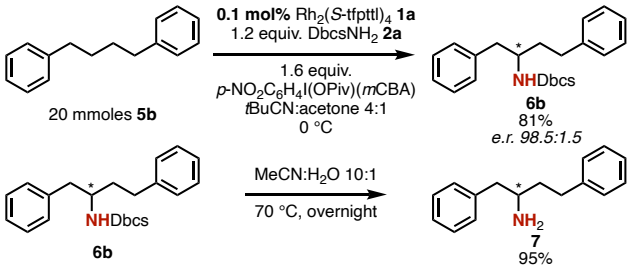

formation of the homobenzylic amines with H:B ratios between 5:1 and 20:1. In each case, the amination of the terminal methylene unit was observed in small to moderate quantities. The formation of this side-product, however, could be suppressed following the introduction of functional groups on the alkyl chain (**4x-4aa**). Particularly worth to mention are the homobenzylic amines **4y-4aa** having a terminal ester group that were isolated almost exclusively with yields ranging from 48% to 71%. This result highlights the synthetic potential of our method for the streamlined synthesis of β- or γ-analogs of phenylalanine derivatives. Importantly, product **4w** showed that the homobenzylic C(sp^3)–H bond can be selectively functionalized in the presence of both a benzylic and a tertiary center.

We also investigated the reactivity of 1,n-arylalkanes **5** (Scheme 7). Remarkably, whereas the reaction using 1,3-diphenylpropane afforded a 1:1 mixture of the benzylic and the homobenzylic amines **6a**, the exclusive formation of the homobenzylic amines **6b** and **6d-e** was observed when using symmetrical 1,4-diarylbutanes. More significantly, a comparable high level of regioselectivity was obtained starting from the non-symmetrical 1,4-diarylbutane **4f** having four non equivalents methylene sites, as a consequence of combined opposite electronic effects on each aromatic ring. Likewise, the reaction with 1,5-diphenylpentane **5c** proved equally regioselective.

The reaction starting from 1,4-diphenylbutane **5b** can be performed with the same efficiency on a 20 mmol scale by using only 0.1 mol% of the rhodium complex **1a** (Scheme 8). Moreover, because the homobenzylic C(sp^3)–H amination reaction involves the use of a chiral dirhodium(II) complex, we evaluated the levels of enantioselectivity for the formation of the amines. Preliminary studies revealed that whereas the homobenzylic products **4a** and **4y** were isolated with enantiomeric ratios of 3:1 and 4:1 respectively, the diphenylbutyl derivative **6b** was obtained nearly enantiopure (e.r. 98.5:1.5). The latter can be deprotected by simple heating in a 10:1 mixture of acetonitrile and water to afford the free amine **7** in 95% yield.

Computational investigations of the mechanism. To propose a rationalization of the selective homobenzylic C(sp^3)–H amination, a DFT study was conducted on the model amination reaction of propylbenzene with $DbcsNH_2$ **2a** as the nitrogen source and Rh_2(*S*-tfpttl)$_4$ **1a** as the catalyst. It is commonly accepted that the active species in the reaction is a metal nitrene intermediate generated upon reaction of the dirhodium catalyst with the sulfamate in the presence of the iodine(III) oxidant.[27-33] However, there is less consensus on the mechanism for the nitrene C–H insertion step which, depending on the system, can proceed by either a concerted transfer, or a stepwise H-abstraction/rebound sequence. Based on physical organic experiments, early work from Du Bois supported a concerted pathway with $Rh_2(esp)_2$ as a catalyst.[5a,25] Such a mechanism was later

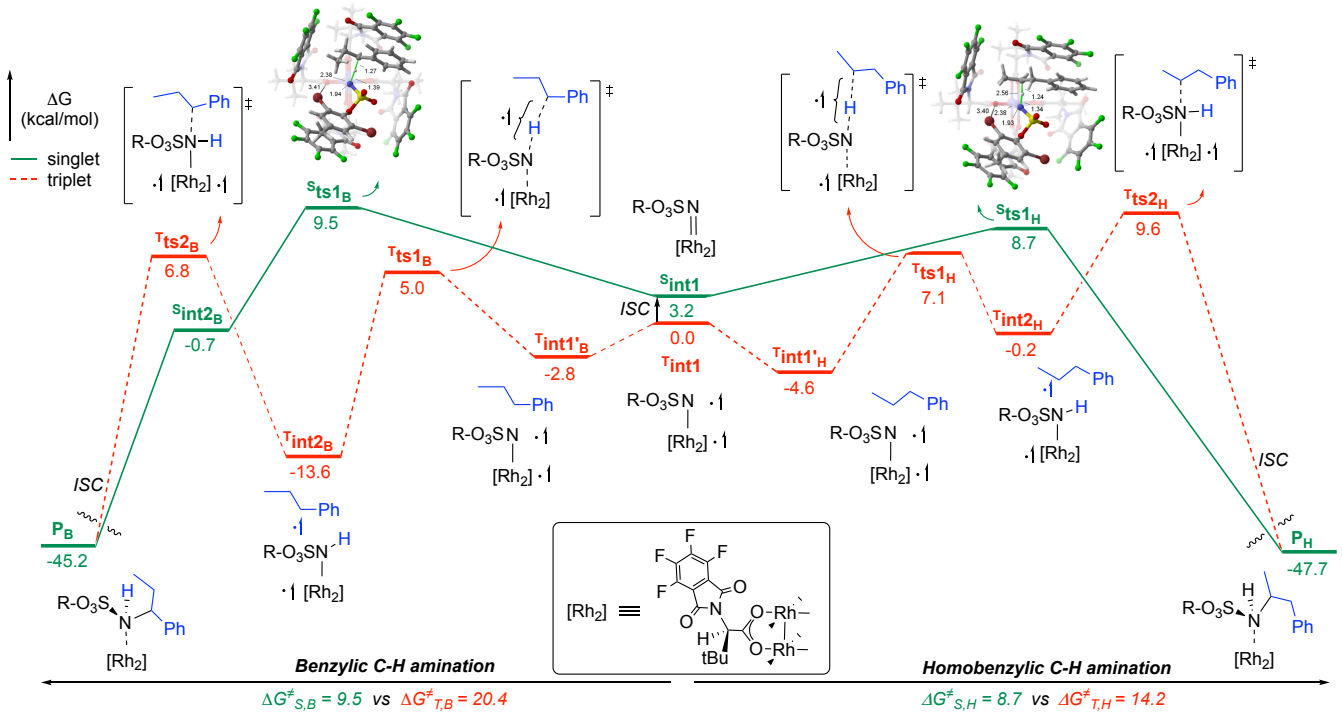

Figure 2. Mechanism of benzylic and homobenzylic C–H amination with the [Rh$_2$]-nitrene (Rh$_2$(*S*-TFPTTL)$_4$ + DbcsNH$_2$) and propylbenzene as a model substrate. The concerted asynchronous pathway is shown in plain green lines, the stepwise in dashed red. Free energies at PCM(t-BuCN)-OPBE-D3(BJ)-def2-tzvp//OPBE-D3(BJ)-def2-svp level of theory, 298K. R = 2,6-dibromophenyl. ISC = intersystem crossing. S = singlet, T = triplet species.

confirmed by the theoretical study performed by Wang to explain the tertiary *vs* benzylic selectivity of intramolecular C–H amination.[29] However, the same study evidenced that a stepwise mechanism is operating in the intermolecular version.[29] Recently, Dang and Liu showed that the Rh$_2$(*S*-*tert*-pttl)$_4$ catalyst was likely to induce diastereoselective C–H amination *via* a triplet stepwise mechanism.[30] These findings suggest that the substrate and catalyst can influence the reactivity pattern, highlighting the need for detailed mechanism examination within our specific system in order to explain the preferential formation of homobenzylic (**P$_H$**) *vs* benzylic (**P$_B$**) C–H amination product.

For both products, we could find a stepwise pathway involving hydrogen abstraction then radical recombination, and an asynchronous concerted pathway for the formation of the C–N bond *via* a unique TS. Their computed Gibbs free energy profiles are shown on Figure 2, in red and green respectively. They feature distinct trends depending on the C–H bond site activated.

The stepwise mechanism starts with the H abstraction from the substrate by the triplet [Rh$_2$]–nitrene species ^{T}**int1**. This step occurs with a lower activation barrier at the benzylic compared to the homobenzylic position (+7.7 kcal/mol *vs* +11.7 kcal/mol respectively) in agreement with their relative BDE (See Table S1). However, the radical ^{T}**int2$_B$** is much more stabilized than ^{T}**int2$_H$**, which can be explained by both its benzylic character and an effect of the catalytic pocket environment (Figure S1). A much higher activation barrier (+20.4 kcal.mol^{-1}) is therefore needed to reach ^{T}**ts2$_B$** and induce the subsequent radical recombination at the benzylic position. On the other hand, rebound at the homobenzylic position operates at a lower cost *via* ^{T}**ts2$_H$** (+9.8 kcal.mol^{-1}). These results show that along the triplet path, distinct steps govern the rate of the stepwise C–H amination. The radical recombination is limiting for the C–H amination at the benzylic position, while it is the H transfer that is decisive for the homobenzylic C–H amination. Furthermore, we observe an overstabilization of the benzylic radical within the catalytic pocket that kinetically disfavors this mechanism in our system.

Alternatively, a concerted path can occur from the energetically accessible singlet nitrene species ^{S}**int1** (+3.2 kcal.mol^{-1}). At the benzylic position, the reaction proceeds via hydride transfer (^{S}**ts1$_B$**, +9.5 kcal.mol^{-1}) to form a stabilized zwitterionic intermediate ^{S}**int2$_B$** (Figure S2) *prior* to C–N bond formation. Subsequently, **P$_B$** is obtained without activation barrier, as indicated by the scan analysis along the C–N bond formation (Figure S3). The scenario is slightly different for the homobenzylic C–H bond amination, which proceeds *via* a concerted asynchronous transition state (^{S}**ts1$_H$**, +8.7 kcal.mol^{-1}) leading directly to the final product **P$_H$**. Again, this difference can be explained by the instability of the homobenzylic cation.

Overall, our calculations show that the concerted mechanism (singlet path) follows a flatter energy profile than the stepwise one (triplet path), and is therefore kinetically favored for the formation of both products. Of note, a two-spin state mechanism was also considered, but the minimum energy crossing points (MECP) found are too high in energy to compete with the singlet mechanism (Table S2 and Figure S4). Accordingly, the –0.8 kcal.mol^{-1} energy difference between ^{S}**ts1$_H$** and ^{S}**ts1$_B$** predicts a H:B discrimination of 4:1 for the C–H amination of propylbenzene, in good agreement with the selectivity obtained experimentally (5.8:1). Several analyses were then performed to interpret the small energy difference between the two ^{S}**ts1** transition states and disclose the key factors controlling this reversed regioselectivity.

kcal/mol	ΔE_{Int}	ΔE_{Pauli}	ΔE_{Elst}	ΔE_{Orb}	ΔE_{Disp}
$^{S}ts_{H}$	-32.7	158.2	-65.6	**-80.0**	-45.2
$^{S}ts_{B}$	-30.2	141.7	-60.7	-66.5	-44.7

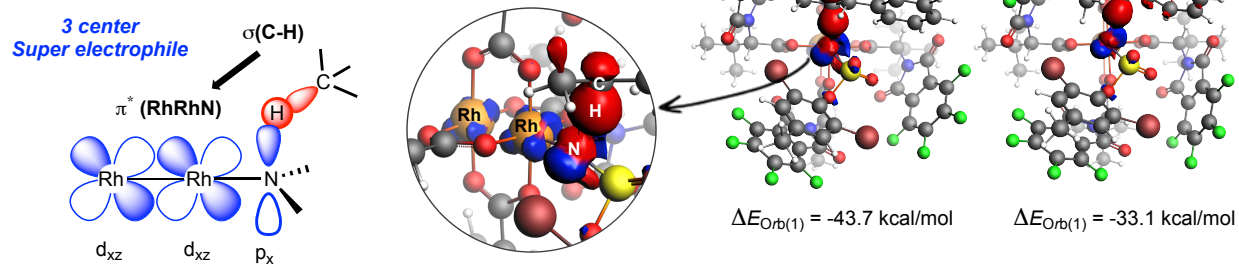

Figure 4. Top left: Comparative energy decomposition analyses for $^{S}ts1_{B}$ and $^{S}ts1_{H}$. Right: Plot of the deformation densities of the main pairwise orbital interactions present in $^{S}ts1_{B}$ and $^{S}ts1_{H}$ and associated stabilization energies $\Delta E_{Orb(1)}$. Bottom left: detail of the main orbitals contributing to this interaction. Data computed at the ZORA-BP86-D3(BJ)/TZ2P//OPBE-D3(BJ)-def2-svp level. Colour code of the charge flow is red → blue and an isosurface value of 0.002 au was used.

Rationalization of the catalyst-controlled regioselectivity by ASM-EDA analysis coupled with steric map and non-covalent interactions plots. A way to assess the impact of the catalytic pocket shape and rigidity on the regioselectivity consists in quantifying the deformation occurring in the substrate and catalyst to reach the transition state geometries ($^{S}ts1_{H}$ and $^{S}ts1_{B}$). This information can be extracted from the activation strain model (ASM) analysis, also known as the distortion/interaction model.[34-38] In this decomposition, the activation energy is split into two terms as shown on Figure 3, with $\Delta E^{\neq}_{strain(X)}$ representing the energy required to distort the reactants (here the substrate and the [Rh_2]–nitrene), and $\Delta E^{\neq}_{int}$ the interaction energy between them.

$$\Delta E^{\ddagger} = [\ \Delta E^{\ddagger}_{strain(Sub)} + \Delta E^{\ddagger}_{strain(Rh)}\ ] + \Delta E^{\ddagger}_{int}$$

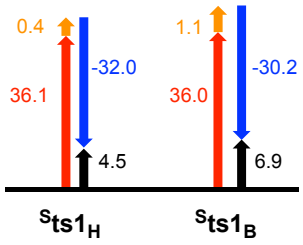

Figure 3. Comparative ASM analysis of the activation energies of the concerted transition states $^{S}ts1_{H}$ and $^{S}ts1_{B}$. Energies (in kcal.mol^{-1}) computed at the PCM(t-BuCN)-OPBE-D3(BJ)-def2-tzvp//OPBE-D3(BJ)-def2-svp level of theory.

At first glance, the two activation energies exhibit similar decomposition trends. Both reveal a pronounced destabilizing strain term for the substrate, a weakly destabilizing strain term for the [Rh_2]–nitrene, and a partially compensating interaction term. The relative order of magnitude of the strain terms reflects a conformational control of the substrate by the catalyst, which is a prerequisite for an efficient site-selectivity.[39]

A first parameter influencing this regiocontrol was evidenced from the slightly smaller strain contribution computed from the [Rh_2]–nitrene fragment in $^{S}ts1_{H}$ compared to $^{S}ts1_{B}$ ($\Delta\Delta E^{\ddagger}_{strain(Rh)}$ = –0.7 kcal.mol^{-1}). This result suggests a better catalytic fit for the homobenzylic activation than the benzylic. Due to the complexity of the [Rh_2]–nitrene geometry, this hypothesis was conveniently corroborated by building the steric map plots of these species (Figure S9), from which the free volume of the catalytic pocket was extracted. Their comparison confirmed a smaller geometric reorganization of the catalyst pocket operating on going from ^{S}**int1** to $^{S}ts1_{H}$ compared to $^{S}ts1_{B}$.

In addition to these subtle differences in the strain terms, a more significant discrimination arises from the interaction term, which is found more stabilizing in the case of $^{S}ts1_{H}$ ($\Delta\Delta E^{\ddagger}_{int}$ = –1.8 kcal.mol^{-1}). Therefore, it appears that the key factor controlling the regioselectivity of the reaction is the degree of interaction between the catalyst and the substrate. In fact, weak interactions were recently described to control the tertiary *vs* benzylic selectivity in rhodium-catalyzed C–H amination with *tert*-butylphenol sulfamate.[40] The tertiary C–H amination was found to be assisted by the establishment of attractive π–π stacking interactions between the substrate and the catalyst, while such non-covalent interactions were absent from the benzylic C–H amination transition state. In our case, the analysis of non-covalent interactions plots featured in $^{S}ts1_{B}$ and $^{S}ts1_{H}$, indicates the presence of stabilizing π–π stacking interactions at both transition states. But additional interactions between the methyl group of propybenzene and the oxygen of an acetate ligand of the catalyst were also found in $^{S}ts1_{H}$ (see Figure S10). To complete this qualitative analysis, and possibly identify other sources of stabilization of $^{S}ts1_{H}$, we decided to perform the Energy Decomposition Analysis (EDA) of the $\Delta E^{\ddagger}_{int}$ term.

This approach allows to split ΔE_{int} into electrostatic interaction (ΔE_{elst}), Pauli repulsion (ΔE_{Pauli}), orbital interaction (ΔE_{orb}) and dispersion energy (ΔE_{disp}) terms.[41,42] The results are tabulated in Figure 4. They confirm that the homobenzylic C–H bond amination displays a higher stabilizing interaction energy due to electrostatic effects ($\Delta\Delta E_{elst}$ = –4.9 kcal.mol^{-1}), but they also reveal that the orbital interaction term plays an even greater role ($\Delta\Delta E_{orb}$ = –13.5 kcal.mol^{-1}). To identify the orbital involved in this interaction, we then applied the Natural Orbital for Chemical Valence (NOCV)[43] analysis. A two-electron donation from the σ(C–H) orbital of the substrate to the π* orbital of the 3-center RhRhN superelectrophile[44] was identified as the dominant contribution to the ΔE_{orb} term in both transition states. However, this interaction is much more stabilizing in the case

of the homobenzylic transition state ($\Delta\Delta E_{orb(1)} = -10.6$ kcal.mol^{-1}), despite a less reactive σ(C–H) orbital. Both a stronger donation of the less elongated homobenzylic C–H bond, suggesting a more concerted transition state; and a better orbital overlap with the LUMO of the [Rh_2]–nitrene electrophile are indeed observed for ^{S}**ts1$_H$**. Hence the favored orbital interaction results from an optimized substrate-catalyst positioning, facilitated by suitable non-covalent interactions.

CONCLUSION

In conclusion, the design of the trisubstituted sulfamate $DbcsNH_2$ **2a** combined with the chiral C_4-symmetrical dirhodium(II) complex Rh_2(*S*-tfpttl)$_4$ **1a** led to a catalytic system enabling an intermolecular homobenzylic C(sp^3)–H amination reaction mediated by an iodine(III) oxidant. This transformation proceeds with a H:B ratio of up to 35:1 and tolerates a wide substrate scope (>30 examples). It can be performed with equal efficiency on a multigram scale by using a rhodium catalyst loading of only 0.1 mol%. Theferore, this method offers a new streamlined access to homobenzylic amines, a motif that builds the core of many biologically active molecules. Preliminary results also show that the homobenzylic amine **6b** derived from 1,4-diphenylbutane can be isolated with a high degree of enantiopurity. To the best of our knowledge, this is a very rare example of an enantioselective amination of an unactivated C(sp^3)–H bond (BDE > 95 kcal.mol^{-1}), as most of the reported methods are limited to the functionalization of activated sites such as benzylic, allylic, or propargylic positions.[12,45] Importantly, for the first time the key influence of the iodoarene part of hypervalent iodine reagents on the efficiency of catalytic nitrene transfers was revealed.

The complete reaction mechanism, involving the concerted and stepwise paths for the homobenzylic *vs* benzylic C–H amination of propylbenzene, was investigated using DFT calculations. The concerted path was identified as the favored mechanism, with the formation of an asynchronous transition state as the key step. As a result, the homobenzylic C–H amination product is kinetically preferred, which is consistent with the experimental observations. According to our ASM-EDA(NOCV) analysis, this is not only due to the slightly relatively lower deformation energy required by the initial [Rh]$_2$–nitrene to adopt the homobenzylic C–H amination transition state structure, but also to the stronger interaction energy establishing between the deformed fragments. The main factor controlling this interaction stems from a stronger orbital interaction between the propylbenzene and the [Rh]$_2$–nitrene complex. Owing to the inherent reactivity of the substrate (B > H) and with the insights from our DFT calculations, we argue that particular non-covalent interactions enable the catalyst to induce a specific orientation of the substrate towards the [Rh]$_2$-nitrene. This orientation, in turn, promotes enhanced orbital overlap in the homobenzylic transition state, thereby favoring the excellent selectivity shift observed experimentally. Taken altogether, these results provide new avenues for the search of rhodium(II)-catalyzed nitrene additions with new selectivities.

ASSOCIATED CONTENT

Supporting Information

The Supporting Information is available free of charge on the ACS Publications website.

Experimental procedures, reaction optimization, characterization data, spectra for all new compounds, HPLC, and details of the computational studies (PDF)

AUTHOR INFORMATION

Corresponding Author

* Philippe Dauban – philippe.dauban@cnrs.fr
* Marie Sircoglou – marie.sircoglou@universite-paris-saclay.fr
* E. Daiann Sosa Carrizo – daiann.sosa-carrizo@universite-paris-saclay.fr

Author Contributions

All authors have given approval to the final version of the manuscript.

Funding Sources

We wish to thank the French National Research Agency (program n° ANR-11-IDEX-0003-02, CHARMMMAT ANR-11-LABX-0039, and ANR-21-CE07-0016-01; fellowship to E. D. S. C.), the Ministère de l'Enseignement Supérieur et de la Recherche (fellowships to V. B. and E. B.), and the ICSN for their support. The computational work was performed using HPC resources from GENCI (Grant 2021-A0070810977).

Notes

The authors declare no competing financial interest.

ACKNOWLEDGMENT

This paper is dedicated to Prof. Erick M. Carreira on the occasion of his 60th birthday.

REFERENCES

(1) (a) Godula, K.; Sames, D. C–H Bond Functionalization in Complex Organic Synthesis. *Science* **2006**, *312*, 67–72. https://doi.org/10.1126/science.1114731 (b) Abrams, D. J.; Provencher, P. A.; Sorensen, E. J. Recent Applications of C–H Functionalization in Complex Natural Product Synthesis. *Chem. Soc. Rev.* **2018**, *47*, 8925-8967. https://doi.org/10.1039/c8cs00716k (c) Chu, J. C. K.; Rovis, T. Complementary Strategies for Directed C(sp^3)–H Functionalization: A Comparison of Transition-Metal-Catalyzed Activation, Hydrogen Atom Transfer, and Carbene/Nitrene Transfer. *Angew. Chem. Int. Ed.* **2018**, *57*, 62–101. https://doi.org/10.1002/anie.201703743 (d) For a seminal study, see: Fraunhoffer, K. J.; Bachovchin, D. A.; White, M. C. Hydrocarbon Oxidation vs C–C Bond-Forming Approaches for Efficient Syntheses of Oxygenated Molecules. *Org. Lett.* **2005**, *7*, 223-226. https://doi.org/10.1021/ol047800p

(2) (a) Cernak, T.; Dykstra, K. D.; Tyagarajan, S.; Vachal, P.; Krska, S. W. The Medicinal Chemist's Toolbox for Late Stage Functionalization of Drug-like Molecules. *Chem. Soc. Rev.* **2016**, *45*, 546–576. https://doi.org/10.1039/C5CS00628G (b) Wencel-Delord, J.; Glorius, F. C–H Bond Activation Enables the Rapid Construction and Late-Stage Diversification of Functional Molecules. *Nat. Chem.* **2013**, *5*, 369–375. https://doi.org/10.1038/nchem.1607

(3) (a) Hartwig, J. F.; Larsen, M. A. Undirected, Homogeneous C–H Bond Functionalization: Challenges and Opportunities. *ACS Cent. Sci.* **2016**, *2*, 281-292. https://doi/org/10.1021/acscentsci.6b00032. (b) White, M. C.; Zhao, J. Aliphatic C–H Oxidations for Late-Stage Functionalization. *J. Am. Chem. Soc.* **2018**, *140*, 13988–14009. https://doi.org/10.1021/jacs.8b05195

(4) (a) Chen, M. S.; White, M. C. A Predictably Selective Aliphatic C–H Oxidation Reaction for Complex Molecule Synthesis. *Science* **2007**, *318*, 783–787. https://doi.org/10.1126/science.1148597. (b) Chen, M. S.; White, M. C. Combined Effects on Selectivity in Fe-Catalyzed Methylene Oxidation. *Science* **2010**, *327*, 566–571. https://doi.org/10.1126/science.1183602 (c) Newhouse, T.; Baran, P.

S. If C–H Bonds Could Talk: Selective C-H Bond Oxidation. *Angew. Chem. Int. Ed.* **2011**, *50*, 3362–3374. https://doi.org/10.1002/anie.201006368 (d) Liao, K.; Negretti, S.; Musaev, D. G.; Bacsa, J.; Davies, H. M. L. Site-Selective and Stereoselective Functionalization of Unactivated C–H Bonds. *Nature* **2016**, *533*, 230–234. https://doi.org/10.1038/nature17651

(5) (a) Fiori, K. W.; Du Bois, J. Catalytic Intermolecular Amination of C−H Bonds: Method Development and Mechanistic Insights. *J. Am. Chem. Soc.* **2007**, *129*, 562–568. https://doi.org/10.1021/ja0650450 (b) Oliva, M.; Coppola, G. A.; Van der Eycken, E. V.; Sharma, U. K. Photochemical and Electrochemical Strategies towards Benzylic C–H Functionalization: A Recent Update. *Adv. Synth. Catal.* **2021**, *363*, 1810-1834. https://doi.org/10.1002/adsc.202001581 (c) Zhang, Y.; Zhang, T.; Das, S. Selective Functionalization of Benzylic C(sp^3)–H Bonds to Synthesize Complex Molecules. *Chem* **2022**, *8*, 3175-3201. https://doi.org/10.1016/j.chempr.2022.10.005

(6) For intermolecular reactions, see: (a) Gormisky, P. E.; White, M. C. Catalyst-Controlled Aliphatic C–H Oxidations with a Predictive Model for Site-Selectivity. *J. Am. Chem. Soc.* **2013**, *135*, 14052–14055. https://doi.org/10.1021/ja407388y (b) Liu, W.; Ren, Z.; Bosse, A. T.; Liao, K.; Goldstein, E. L.; Bacsa, J.; Musaev, D. G.; Stolz, B. M.; Davies, H. M. L. Catalyst-Controlled Selective Functionalization of Unactivated C–H Bonds in the Presence of Electronically Activated C–H Bonds. *J. Am. Chem. Soc.* **2018**, *140*, 12247–12255. https://doi.org/10.1021/jacs.8b07534. (c) Bakhoda, A.; Jiang, Q.; Badiei, Y. M.; Bertke, J. A.; Cundari, T. R.; Warren, T. H. Copper-Catalyzed C(sp^3)−H Amidation: Sterically Driven Primary and Secondary C−H Site-Selectivity. *Angew. Chem. Int. Ed.* **2019**, *58*, 3421–3425. https://doi.org/10.1002/anie.201810556 For intramolecular reactions, see: (d) Fiori, K. W.; Espino, C. G.; Brodsky, B. H.; Du Bois, J. A Mechanistic Analysis of the Rh-Catalyzed Intramolecular C–H Amination Reaction. *Tetrahedron* **2009**, *65*, 3042–3051. https://doi.org/10.1016/j.tet.2008.11.073 (e) Taber, D. F.; Ruckle Jr., R. E. Cyclopentane Construction by $Rh_2(OAc)_4$-Mediated Intramolecular C–H Insertion: Steric and Electronic Effects. *J. Am. Chem. Soc.* **1986**, *108*, 7686-7693. https://doi.org/10.1021/ja00284a037

(7) (a) Gillespie, J. E.; Fanourakis, A.; Phipps, R. J. Strategies that Utilize Ion Pairing Interactions to Exert Selectivity Control in the Functionalization of C–H Bonds. *J. Am. Chem. Soc.* **2022**, *144*, 18195-18211. https://doi.org/10.1021/jacs.2c08752 (b) Jiao, Y.; Chen, X.-Y.; Stoddart, J. F. Weak Bonding Strategies for Achieving Regio- and Site-Selective Transformations. *Chem* **2022**, *8*, 414-438. https://doi.org/10.1016/j.chempr.2021.12.012

(8) (a) Breslow, R.; Huang, Y.; Zhang, X.; Yang, J. An Artificial Cytochrome P450 that Hydroxylates Unactivated Carbons with Regio- and Stereoslectivity and Useful Catalytic Turnovers. *Proc. Natl. Acad. Sci USA* **1997**, *94*, 11156-11158. https://doi.org/10.1073/pnas.94.21.11156 (b) Breslow, R.; Rajagopalan, R. Schwarz, J. Selective Functionalization of Doubly Coordinated Flexible Chains. *J. Am. Chem. Soc.* **1981**, *103*, 2905-2907. https://doi.org/10.1021/ja00400a088 (c) Breslow, R.; Winnik, M. A. Remote Oxidation of Unactivated Methylene Groups. *J. Am. Chem. Soc.* **1969**, *91*, 3083-3084. https://doi.org/10.1021/ja01039a043

(9) For reviews, see: (a) Hartwig, J. F. Catalyst-Controlled Site-Selective Bond Activation. *Acc. Chem. Res.* **2017**, *50*, 549–555. https://doi.org/10.1021/acs.accounts.6b00546 (b) Vidal, D.; Olivo, G.; Costas, M. Controlling Selectivity in Aliphatic C–H Oxidations through Supramolecular Recognition. *Chem. Eur. J.* **2018**, *24*, 5042-5054. https://doi.org/10.1002/chem.201704852 For relevant examples, see: (c) Das, S.; Incarvito, C. D.; Crabtree, R. H.; Brudvig, G. W. Molecular Recognition in the Selective Oxygenation of Saturated C–H Bonds by a Dimanganese Catalyst. *Science* **2006**, *312*, 1941-1943. https://doi.org/10.1126/science.1127899 (d) Burg, F.; Gicquel, M.; Breitenlechner, S.; Pöthig, A.; Bach, T. Site- and Enantioselective C–H Oxygenation Catalyzed by a Chiral Manganese Porphyrin Complex with a Remote Binding Site. *Angew. Chem. Int. Ed.* **2018**, *57*, 2953-2957. https://doi.org/10.1002/anie.201712340

(10) (a) Olivo, G.; Farinelli, G.; Barbieri, A.; Lanzalunga, O.; Di Stefano, S.; Costas, M. Supramolecular Recognition Allows Remote, Site-Selective C–H Oxidation of Methylene Sites in Linear Amines. *Angew. Chem. Int. Ed.* **2017**, *56*, 16347-16351. https://doi.org/10.1002/anie.201709280 (b) Olivo, G.; Capocasa, G.; Lanzalunga, O.; Di Stefano, S.; Costas, M. Enzyme-Like Substrate-Selectivity in C–H Oxidation Enabled by Recognition. *Chem. Commun.* **2019**, *55*, 917-920. https://doi.org/10.1039/c8cc09328h (c) Knezevic, M.; Heilmann, M.; Piccini, G. M.; Tiefenbacher, K. Overriding Intrinsic Reactivity in Aliphatic C–H Oxidation: Preferential C3/C4 Oxidation of Aliphatic Ammonium Substrates. *Angew. Chem. Int. Ed.* **2020**, *59*, 12387-12391. https://doi.org/10.1002/anie.2020004242 (d) Knezevic, M.; Tiefenbacher, K. Tweezer-Based C–H Oxidation Catalysts Overriding Intrinsic Reactivity of Aliphatic Ammonium Substrates. *Chem. Eur. J.* **2023**, *29*, e202203480. https://doi.org/10.1002/chem.202203480

(11) (a) Höke, T.; Herdtweck, E.; Bach, T. Hydrogen-Bond Mediated Regio- and Enantioselectivity in a C–H Amination Reaction Catalyzed by a Supramolecular Rh(II) Complex. *Chem. Commun.* **2013**, *49*, 8009-8011. https://doi.org/10.1039/c3cc44197k (b) Annapureddy, R. R.; Jandl, C.; Bach, T. A Chiral Phenanthroline Ligand with a Hydrogen-Bonding Site: Application to the Enantioselective Amination of Methylene Groups. *J. Am. Chem. Soc.* **2020**, *142*, 7374-7378. https://doi.org/10.1021/jacs.0c02803 (c) Fanourakis, A.; Williams, B. D.; Paterson, K. J.; Phipps, R. J. Enantioselective Intermolecular C–H Amination Directed by a Chiral Cation. *J. Am. Chem. Soc.* **2021**, *143*, 10070-10076. https://doi.org/10.1021/jacs.1c05206

(12) For reviews, see: (a) Roizen, J. L.; Harvey, M. E.; Du Bois, J. Metal-Catalyzed Nitrogen-Atom Transfer Methods for the Oxidation of Aliphatic C–H Bonds. *Acc. Chem. Res.* **2012**, *45*, 911–-922. https://doi.org/10.1021/ar200318q (b) Darses, B.; Rodrigues, R.; Neuville, L.; Mazurais, M.; Dauban, P. Transition Metal-Catalyzed Iodine(III)-Mediated Nitrene Transfer Reactions: Efficient Tools for Challenging Syntheses. *Chem. Commun.* **2017**, *53*, 493–508. https://doi.org/10.1039/C6CC07925C (c) Hazelard, D.; Nocquet, P.-A.; Compain, P. Catalytic C–H Amination at its Limits: Challenges and Solutions. *Org. Chem. Front.* **2017**, *4*, 2500–2521. https://doi.org/10.1039/c7qo00547d (d) Ju, M.; Schomaker, J. Nitrene Transfer Catalysts for Enantioselective C–N Bond Formation. *Nat. Rev. Chem.* **2021**, *5*, 580-594. https://doi.org/10.1038/s41570-021-00291-4 For relevant examples of catalytic benzylic C(sp^3)–H amination, see: (e) Nishioka, Y.; Uchida, T.; Katsuki, T. Enantio- and Regioselective Intermolecular Benzylic and Allylic C–H Bond Amination *Angew. Chem. Int. Ed.* **2013**, *52*, 1739–1742. https://doi.org/10.1002/anie.201208906 (f) Bess, E. N.; DeLuca, R. J.; Tindall, D. J.; Oderinde, M. S.; Roizen, J. L.; Du Bois, J.; Sigman, M. S. Analyzing Site Selectivity in $Rh_2(esp)_2$-Catalyzed Intermolecular C–H Amination Reactions. *J. Am. Chem. Soc.* **2014**, *136*, 5783–5789. https://doi.org/10.1021/ja5015508 (g) Buendia, J.; Darses, B.; Dauban, P. Tandem Catalytic C(sp^3)–H Amination/Sila-Sonogashira-Hagihara Coupling Reactions with Iodine Reagents. *Angew. Chem. Int. Ed.* **2015**, *54*, 5697–5701. https://doi.org/10.1002/anie.201412364 (h) Clark, J. R.; Feng, K.; Sookezian, A.; White, M. C. Manganese-Catalysed Benzylic C(sp^3)–H Amination for Late-Stage Functionalization. *Nat. Chem.* **2018**, *10*, 583–591. https://doi.org/10.1038/s41557-018-0020-0

(13) Rare examples of intramolecular homobenzylic C(sp^3)–H amination reactions with a very limited scope were previously reported. see: (a) Ruppel, J. V.; Kamble, R. M.; Zhang, X. P. Cobalt-Catalyzed Intramolecular C–H Amination with Arylsulfonyl Azides. *Org. Lett.* **2007**, *9*, 4889-4892. https://doi.org/10.1021/ol702265h (b) Hyster, T. K.; Farwell, C. C.; Buller, A. R.; McIntosh, J. A.; Arnold, F. H. Enzyme-Controlled Nitrogen-Atom Transfer Enables Regiodivergent C–H Amination. *J. Am. Chem. Soc.* **2014**, *136*, 15505-15508. https://doi.org/10.1021/ja509308v (c) Scamp, R. J.; Scheffer, B.; Schomaker, J. M. Regioselective Differentiation of Vicinal Methylene C–H Bonds Enabled by Silver-Catalyzed Nitrene Transfer. *Chem. Commun.* **2019**, *55*, 7362-7365. https://doi.org/10.1039/c9cc04006d

(14) Freeman, S.; Alder, J. F. Arylethylamine psychotropic recreational drugs: a chemical perspective. *Eur. J. Med. Chem.* **2002**, *37*, 527-539. https://doi.org/10.106/s0223-5234(02)01382-x

(15) (a) *Chiral Amine Synthesis. Methods, Developments and Applications*; Nugent, T. C., Ed.; Wiley-VCH, Weinheim, **2010**. (b) Boyington, A. J.; Seath, C. P.; Zearfoss, A. M.; Xu, Z.; Jui, N. T. Catalytic Strategy for Regioselective Arylethylamine Synthesis. *J. Am. Chem. Soc.* **2019**, *141*, 4147-4153. https://doi.org/10.1021/jacs.9b01077 (c)

Trowbridge, A.; Walton, S. M.; Gaunt, M. J. New Strategies for the Transition-Metal Catalyzed Synthesis of Aliphatic Amines. *Chem. Rev.* **2020**, *120*, 2613-2692. https://doi.org/10.1021/acs.chemrev.9b00462

(16) (a) Davies, H. M. L.; Liao, K. Dirhodium Tetracarboxylates as Catalysts for Selective Intermolecular C–H Functionalization. *Nat. Rev. Chem.* **2019**, *3*, 347–360. https://doi.org/10.1038/s41570-019-0099-x (b) Buendia, J.; Grelier, G.; Dauban, P. Dirhodium(II)-Catalyzed C(sp^3)–H Amination Using Iodine(III) Oxidants. *Adv. Organomet. Chem.* **2015**, *64*, 77–118. https://dx.doi.org/10.1016/bs.adomc.2015.08.001

(17) (a) Roizen, J. L.; Zalatan, D. N.; Du Bois, J. Selective Intermolecular Amination of C–H Bonds at Tertiary Carbon Centers. *Angew. Chem. Int. Ed.* **2013**, *52*, 11343–11346. https://doi.org/10.1002/anie.201304238 (b) Chiappini, N. D.; Mack, J. B. C.; Du Bois, J. Intermolecular C(sp^3)−H Amination of Complex Molecules. *Angew. Chem. Int. Ed.* **2018**, *57*, 4956–4959. https://doi.org/10.1002/anie.201713225 (c) Nasrallah, A.; Boquet, V.; Hecker, A.; Retailleau, P.; Darses, B.; Dauban, P. Catalytic Enantioselective Intermolecular Benzylic C(sp^3)−H Amination. *Angew. Chem. Int. Ed.* **2019**, *58*, 8192–8196. https://doi.org/10.1002/anie.201902882 (d) Nasrallah, A.; Lazib, Y.; Boquet, V.; Darses, B.; Dauban, P. Catalytic Intermolecular C(sp^3)–H Amination with Sulfamates for the Asymmetric Synthesis of Amines. *Org. Process. Res. Dev.* **2020**, *24*, 724-728. https://doi.org/10.1021/acs.oprd.9b00424 (e) Brunard, E.; Boquet, V.; Van Elslande, E.; Saget, T.; Dauban, P. Catalytic Intermolecular C(sp^3)–H Amination: Selective Functionalization of Tertiary C–H Bonds *vs.* Activated Benzylic C−H Bonds. *J. Am. Chem. Soc.* **2021**, *143*, 6407-6412. https://doi.org/10.1021/jacs.1c03872

(18) Boquet, V.; Nasrallah, A.; Dana, A. L.; Brunard, E.; Di Chenna, P. H.; Duran, F. J.; Retailleau, P.; Darses, B.; Sircoglou, M.; Dauban, P. Rhodium(II)-Catalyzed Enantioselective Intermolecular Aziridination of Alkenes *J. Am. Chem. Soc.* **2022**, *144*, 17156-17164. https://doi.org/10.1021/jacs.2c07337

(19) McKillop, A.; Kemp, D. Further Functional Group Oxidations Using Sodium Perborate. *Tetrahedron* **1989**, *45*, 3299-3306. https://doi.org/10.1016/S0040-4020(01)81008-5

(20) Watanabe, A.; Miyamoto, K.; Okada, T.; Asawa, T.; Uchiyama, M. Safer Synthesis of (Diacetoxyiodo)arenes Using Sodium Hypochlorite Pentahydrate. *J. Org. Chem.* **2018**, *83*, 14262-14268. https://doi.org/10.1021/acs.joc.8b02541

(21) Iinuma, M.; Moriyama, K.; Togo, H. Simple and Practical Method for the Preparation of (Diacetoxy)iodoarenes with Iodoarenes and *m*-Chloroperoxybenzoic Acid. *Synlett* **2012**, *23*, 2663-2666. https://doi.org/10.1055/s-0032-1317345

(22) (a) Zalatan, D. N.; Du Bois, J. Understanding the Differential Performance of $Rh_2(esp)_2$ as a Catalyst for C–H Amination. *J. Am. Chem. Soc.* **2009**, *131*, 7588-7559. https://doi.org/10.1021/ja902893u (b) Roizen, J. L; Zalatan, D. N.; Du Bois, J. Selective Intermolecular Amination of C–H Bonds at Tertiary Carbon Centers. *Angew. Chem. Int. Ed.* **2013**, *52*, 11343-11346. https://dx.doi.org/10.1002/anie.201304238

(23) The iodoarene moiety of a trivalent iodine reagent was shown to influence the diastereoselectivity of a cyclization performed from electrophilic *N*-aryl nitrenoids. See: Deng, T.; Shi, E.; Thomas, E.; Driver, T. G. I(III)-Catalyzed Oxidative Cyclization-Migration Tandem Reactions of Unactivated Anilines. *Org. Lett.* **2020**, *22*, 9102-9106. https://doi.org/10.1021/acs.orglett.0c03497

(24) Li, Z.; Quan, R. W.; Jacobsen, E. N. Mechanism of the (Diimine)copper-Catalyzed Asymmetric Aziridination of Alkenes. Nitrene Transfer via Ligand-Accelerated Catalysis. *J. Am. Chem. Soc.* **1995**, *117*, 5889-5890. https://doi.org/10.1021/ja00126a044

(25) Perry, R.H.; Cahill III, T. J.; Roizen, J. L.; Du Bois, J.; Zare, R. N. Capturing fleeting intermediates in a catalytic C–H amination reaction cycle. *Proc Natl Acad Sci.* **2012**, *109*, 18295–18299. https://doi.org/10.1073/pnas.1207600109

(26) An initial screening of solvents revealed the compatibility of acetone or *i*-propyl acetate with the homobenzylic C–H amination reaction. This result proved helpful to study the reaction at temperatures below 15 °C, which is the melting point of pivalonitrile. Moreover, it is worth mentioning that using 1.6 equivalent of the *p*-$NO_2C_6H_4I(OPiv)_2$ reagent under these conditions led to the isolation of the homobenzylic amine in a slightly reduced yield of 87%. This result gave support to our previous choice for the hypervalent iodine reagent discussed in scheme 4. Finally, the red color typical of the Rh(II)/(Rh(III) species resulting from the oxidation of the dirhodium(II) complex, is never observed under these conditions.

(27) Lorpitthaya, R.; Xie, Z. Z.; Sophy, K. B.; Kuo, J. L.; Liu, X. W. Mechanistic Insights into the Substrate-Controlled Stereochemistry of Glycals in One-Pot Rhodium-Catalyzed Aziridination and Aziridine Ring Opening. *Chem. - A Eur. J.* **2010**, *16*, 588–594. https://doi.org/10.1002/chem.200901727.

(28) Wang, J.; Zhao, C.; Weng, Y.; Xu, H. Insight into the Mechanism and Site-Selectivity of Rh2II,II(Esp)2-Catalyzed Intermolecular C-H Amination. *Catal. Sci. Technol.* **2016**, *6*, 5292–5303. https://doi.org/10.1039/c6cy00505e

(29) Wang, J.; Zheng, K.; Lin, B.; Weng, Y. A Comparative Study of Inter- and Intramolecular C-H Aminations: Mechanism and Site Selectivity. *RSC Adv.* **2017**, *7*, 34783–34794. https://doi.org/10.1039/c7ra05032a

(30) Li, Q.; Liu W.; .Dang Y. Origins of ligand-controlled diastereoselectivity in dirhodium-catalysed direct amination of aliphatic C(sp^3)–H bonds. *Catal. Sci. Technol.* **2021**, *11*, 6960–6964. https://doi.org/10.1039/d1cy01583d

(31) Kono, M.; Harada, S.; Nemoto, T. Chemoselective Intramolecular Formal Insertion Reaction of Rh–Nitrenes into an Amide Bond Over C−H Insertion. *Chem. - A Eur. J.* **2019**, *25*, 3119–3124. https://doi.org/10.1002/chem.201805878

(32) Azek, E.; Khalifa, M.; Bartholoméüs, J.; Ernzerhof, M.; Lebel, H. Rhodium(Ii)-Catalyzed C-H Aminations Using N -Mesyloxycarbamates: Reaction Pathway and by-Product Formation. *Chem. Sci.* **2019**, *10*, 718–729. https://doi.org/10.1039/c8sc03153c

(33) Noda, H.; Tang, X.; Shibasaki, M. Catalyst-Controlled Chemoselective Nitrene Transfers. *Helv. Chim. Acta* **2021**, *104*. https://doi.org/10.1002/hlca.202100140

(34) Fernández, I.; Bickelhaupt, F. M. The Activation Strain Model and Molecular Orbital Theory: Understanding and Designing Chemical Reactions. *Chem. Soc. Rev.* **2014**, *43*, 4953–4967. https://doi.org/10.1039/C4CS00055B

(35) Wolters, L. P.; Bickelhaupt, F. M. The Activation Strain Model and Molecular Orbital Theory. *WIREs Comput. Mol. Sci.* **2015**, *5*, 324–343. https://doi.org/10.1002/wcms.1221

(36) Bickelhaupt, F. M.; Houk, K. N. Analyzing Reaction Rates with the Distortion/Interaction-Activation Strain Model. *Angew. Chemie - Int. Ed.* **2017**, *56*, 10070–10086. https://doi.org/10.1002/anie.201701486

(37) Sosa Carrizo, E. D.; Bickelhaupt, F. M.; Fernández, I. Factors Controlling β-Elimination Reactions in Group 10 Metal Complexes. *Chem. - A Eur. J.* **2015**, *21*, 14362–14369. https://doi.org/10.1002/chem.201502036

(38) Bonnin, Q.; Edlová, T.; Sosa Carrizo, E. D.; Fleurat-Lessard, P.; Brandès, S.; Cattey, H.; Richard, P.; Le Gendre, P.; Normand, A. T. Coordinatively Unsaturated Amidotitanocene Cations with Inverted σ and π Bond Strengths: Controlled Release of Aminyl Radicals and Hydrogenation/Dehydrogenation Catalysis. *Chem. - A Eur. J.* **2021**, *27*, 18175–18187. https://doi.org/10.1002/chem.202103487

(39) In agreement with these values, we found a considerable flattening of propylbenzene in the transition state (Figure S5), while the [Rh_2]–nitrene pocket remains preorganized. This, and complementary analyses detailed in the supporting information (Figures S6, S7, and S8) give support to the conformational control of the substrate by the catalyst.

(40) Su, X.-X.; Chen, X.-H.; Ding, D.-B.; She, Y.-B.; Yang, Y.-F. Computational Exploration of Dirhodium Complex-Catalyzed Selective Intermolecular Amination of Tertiary vs. Benzylic C-H Bonds. *Molecules* **2023**, *28*, 1928. https://doi.org/10.3390/molecules28041928

(41) Bickelhaupt, F. M.; Baerends, E. J. Kohn-Sham Density Functional Theory: Predicting and Understanding Chemistry. *Rev. Comput. Chem.* **2000**, *15*, 1–86. https://doi.org/10.1002/9780470125922.ch1

(42) Hopffgarten, M. von; Frenking, G. Energy Decomposition Analysis. *Wiley Interdiscip. Rev. Comput. Mol. Sci.* **2017**, *8*, 1–39. https://doi.org/10.1002/wcms.71

(43) Mitoraj, M. P.; Michalak, A.; Ziegler, T. A Combined Charge and Energy Decomposition Scheme for Bond Analysis. *J. Chem. Theory Comput.* **2009**, *5*, 962–975. https://doi.org/10.1021/ct800503d

(44) Berry, J. F. The Role of Three-Center/Four-Electron Bonds in Superelectrophilic Dirhodium Carbene and Nitrene Catalytic Intermediates. *Dalton Trans.* **2012**, 700–713. https://doi.org/10.1039/c1dt11434d

(45) For a recent example of enantioselective amination of unactivated C–H bonds, see: Athavale, S. V.; Gao, S.; Das, A.; Mallojjala, S. C.; Alfonzo, E.; Long, Y.; Hirschi, J. S.; Arnold, F. H. Enzymatic Nitrogen Insertion into Unactivated C–H Bonds. *J. Am. Chem. Soc.* **2022**, *144*, 19097-19105. https://doi.org/10.1021/jacs.2c08285

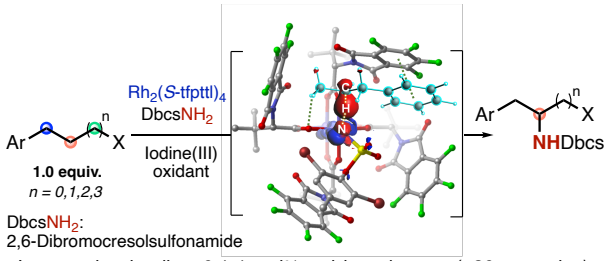

DbcsNH$_2$:
2,6-Dibromocresolsulfonamide

- *Low catalyst loading: 0.1-1 mol%* and *broad scope (>30 examples)*
- *Yields up to 90% and* ***Homobenzylic:Benzylic*** *ratio of up to* ***35:1***
- *Regioselectivity through specific non-covalent and orbital interactions*